Proceedings of the 1999 IEEE/RSJ
International Conference on
Intelligent Robots and Systems

Bio-mimetic Trajectory Generation of Robots using Time Base Generator

Yoshiyuki Tanaka Toshio Tsuji Makoto Kaneko
Faculty of Engineering, Hiroshima University
Higashi-Hiroshima, 739-8527 Japan

Abstract

In this paper, the human-like trajectory of robots for manipulating a holding nonholonomic car is generated. In order to reveal what kind of trajectories the robots should generate on the task, the experiments with subjects were performed. Then, it is shown that a human generates the trajectories with a single-peaked and a double-peaked velocity profile. By modeling these primitive profiles with a Time Base Generator (TBG), the human-like trajectory for the robots is generated with the TBG based trajectory generation method. Finally, simulation results are shown and compared with the human trajectories.

Key Words: Human movements, trajectory generation, nonholonomic constraints, TBG.

1 Introduction

The development of a human-shaped robot has been actively performed [1], so that a friendly feeling of a human toward the robot is practically realized from a cosmetic point of view. However, no matter how similar to a human only in appearance the robot is, it will not be able to cowork or coexsit with human beings in a daily life if it cannot move or perform a given task with human-like movements.

On the other hand, there have been many studies on the mechanism of human arm movements [2]-[6]. For instance, Morasso [2] measured reaching movements of the two-joint arm restricted to an horizontal plane, and found the common invariant kinematic features that a human usually moves his hand along a roughly straight path with a bell-shaped velocity profile from one point to another. As the explanation for the trajectory generation mechanism of this human arm movement, many models have been proposed; for example, "a minimum jerk model" [3], "a minimum torque-change model" [4] and "a VITE model" [5]. The first and the second model asserts that the mechanism is a feed-forward system, and the other deals it as a feedback system. All of these models can generate hand trajectories in good agreement with experimental data.

Also, Morasso et al. [6] proposed a Time Base Generator (TBG) which generates a time-series with a bell-shaped velocity profile, and showed that a straight and a curved hand trajectory can be generated by synchronizing a translational and a rotational velocity of the hand with the TBG signal. Then, Tsuji et al. [7] [8] applied the TBG to the control of a nonholonomic robot and a redundant manipulator. Moreover, Tanaka et al. [9] developed a trajectory generation method based on the artificial potential field approach with the combination of time scale transformation and the TBG. These previous studies, however, have not handle the trajectory generation with any constraints, although a human movement is often constrained by environments on performing an ordinary work in a daily life.

Recently, Tanaka et al. [10] have focused on the trajectory generation on the nonholonomic constrained task which is the manipulation of a holding nonholonomic vehicle from a point to another, and revealed that a human generates the trajectory with a single-peaked or a double-peaked velocity profile through the experiments with subjects. Then, by modeling these primitive profiles with the TBG, the trajectories which have the same features of the human ones can be reproduced except for the complicated trajectory such a trajectory including a switching point. In the present paper, the human-like trajectory including the switching one for the robots on the nonholonomic constrained task is generated by regulating a temporal profile of the TBG.

This paper is organized as follows: Section 2 describes the characteristics of human trajectories generated on the nonholonomic constrained task. In section 3, a feedback controller to reproduce the observed human hand trajectories is designed by means of the TBG based method. Finally, the simulation results are shown and compared with the human trajectories in Section 4.

2 Human arm movements with nonholonomic constraints

2.1 Experimental conditions

Figure 1 shows an experimental apparatus. A subject is instructed to sit on his heels and move the holding nonholonomic model car which has two wheels and one spherical wheel as shown in Fig. 1 (b) from an initial point marked with □ to a target point ◇ on a specified condition (see Fig. 1 (a)). In the experiment, the translational velocity v and the angular velocity ω of the model car are calculated as human hand velocities by measuring movements of the model car and the subject's arm with a stereo camera system (Quick MAG, OUYOU KEISOKU KENKYUSYO INC.).

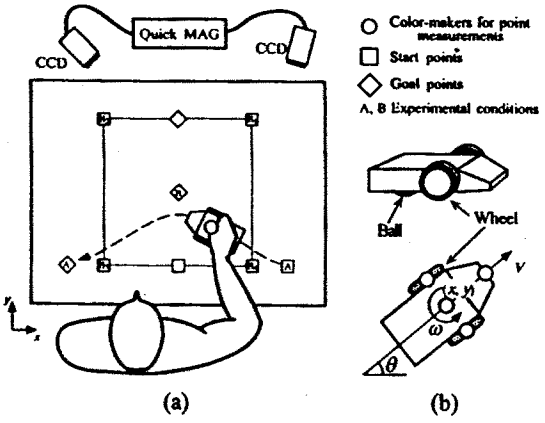

Fig.1 Experimental apparatus

The camera system can detect a 3-D position of a color marker (marked with ○ in Fig. 1 (b)) attached at a point of measurement, maximum of 8 points, from two 2-D image sequences taken by two CCD cameras in real time. Both v and ω were calculated through the digital differentiation of the smoothed marker's positional data where the cut-off frequency of the second-order Butterworth filter is automatically determined with Winter's method [11]. With this apparatus, the experiments was carried out with the following contidions (see Fig. 1 (a)):

A: Move the model car from the initial point Ⓐ to the target point ◈ with the initial posture $\theta_0 = \pi$[rad] and the target posture $\theta_d = \pi$[rad] in the generalized coordinates Σ_b. Also, the subject is asked to generate a vertically curved spatial trajectory like the dotted line shown in Fig. 1 (a) as the trials goes on.

B: Move the model car from the initial points Ⓑ$_i$ $(i = 1, \cdots, 4)$ to the target point ◈ under the initial posture $\theta_0 = \frac{\pi}{2}$[rad] and the target posture $\theta_d = \pi$[rad]. The initial points are located at the vartexes of a square whose sides are 400 [mm] long and the target point is positioned at the center of the square.

In the experiments, the number of subjects was three (male university students aged 22, 23 and 28), and the order of the experimental conditions and the number of trials were changed for each subject.

2.2 Generated trajectories

Figure 2 shows a typical example of the observed spatial trajectories and translational velocity profiles of the model car, where the translational velocity v is normalized by its maximum velocity v_{max} and the time t by the measured movement time t_f from the initial point to the target for each trials.

It can be seen that the straight trajectories have single-peaked velocity profiles which peaks around $t = \frac{t_f}{2}$ as shown in Fig. 2 (a). Also, it should be noticed that as the amplitude of the curvature is lager,

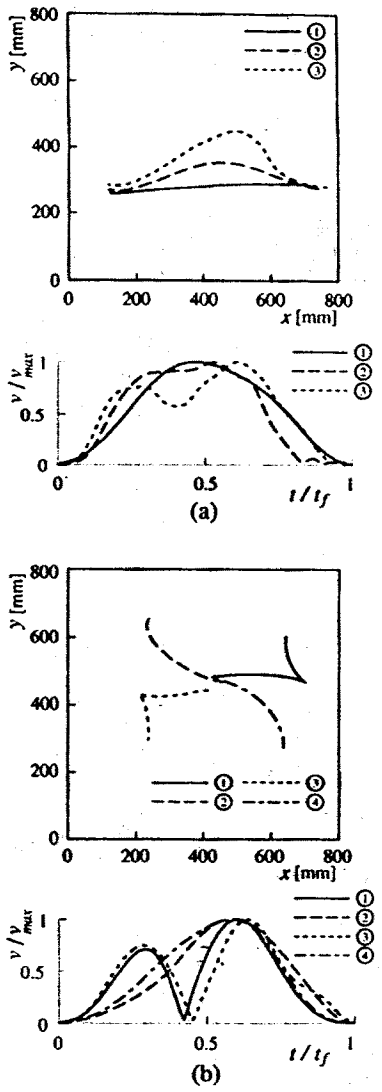

Fig.2 Generated spatio-temporal trajectories under the different experimental conditions

the velocity profile tends to be more sharply double-peaked.

On the other hand, under the experimental condition B, the subjects generated two kinds of spatial trajectories according to the specified initial point as shown in Fig. 2 (b): the trajectory including one switching point, and the quadrantal-arc trajectory. It can be observed that the quadrantal-arc trajectories have the single-peaked velocity profiles and the others the coupled-profiles with two single-peaked ones. Also, from features of the generated switching trajectories, it can be suggested that a switching trajectory is produced as the result of connecting a straight line with a quadrantal arc at the switching point.

Summing up, the following features of the human hand trajectories on the task were observed as:

1) The subjects generates two types of the primitive velocity profiles: the single-peaked profile and the double-peaked one.

2) The subjects generates the different spatial trajectories according to the initial point and the target one.

3) The subjects generates a velocity profile out of two primitive ones according to the generated spatial trajectory.

3 Trajectory generation based on Time Base Generator

In the previous section, the human primitive movements on the manipulation of the nonholonomic model car was revealed. Here, a method for generating the human-like trajectories is described.

Tanaka et al. [9] have developed the trajectory generation method for a robot based on the artificial potential field approach (APFA) with the combination of a time scale transformation and a time base generator (TBG) [6]. Then, they [10] applied it to reproduce the primitive human trajectories, which dose not have a switching point, on the nonholonomic constrained task. In this paper, the human-like trajectories for the robots including switching ones on the nonholonomic constrained task is generated by using the TBG based method.

3.1 Virtual time and the TBG

First, we define a virtual time s for time scaling the system. The relationship between actual time t and virtual time s is given by

$$\frac{ds}{dt} = a(t)\,, \tag{1}$$

where the continuous function $a(t)$, called the time scale function [12], is defined as follows:

$$a(t) = -p\frac{\dot{\xi}}{\xi}\,, \tag{2}$$

where p is a positive constant and $\xi(t)$ is a non-increasing function generated by the TBG [7] [8]. $\xi(t)$ has a bell-shaped velocity profile satisfying $\xi(0) = 1$ and $\xi(t_f) = 0$ with the convergence time t_f. The dynamics of ξ is defined as follows:

$$\dot{\xi} = -\gamma\xi^{\beta_1}(1-\xi)^{\beta_2}, \tag{3}$$

where γ and β_i $(i = 1, 2)$ are positive constants under $0 < \beta_i < 1$. The temporal profile of the TBG can be adjusted by changing the parameters β_i. Then, the convergence time t_f can be calculated with the gamma function $\Gamma(\,\cdot\,)$ as

$$t_f = \int_0^{t_f} dt = \frac{\Gamma(1-\beta_1)\Gamma(1-\beta_2)}{\gamma\Gamma(2-(\beta_1+\beta_2))}. \tag{4}$$

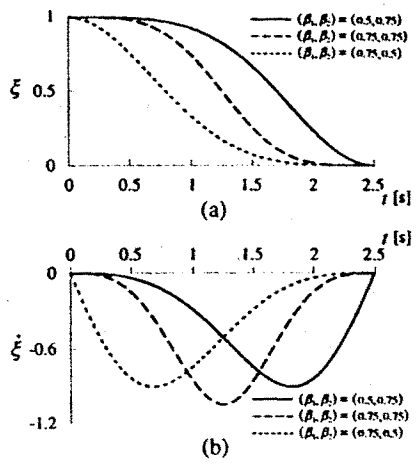

Fig.3 Dynamic behavior of the TBG

Thus, the system converges to the equilibrium point $\xi = 0$ in the finite time t_f if the parameter γ is chosen as

$$\gamma = \frac{\Gamma(1-\beta_1)\Gamma(1-\beta_2)}{t_f\Gamma(2-(\beta_1+\beta_2))}. \tag{5}$$

Figure 3 shows the time histories of ξ and $\dot{\xi}$ under the parameter $(\beta_1,\ \beta_2) = (0.75,\ 0.5)$, $(0.75,\ 0.75)$, $(0.5,\ 0.75)$ with the convergence time $t_f = 2.5$ [s].

From (1) and (2), virtual time s can be derived as follows:

$$s = \int_0^t a(t)\,dt = -p\ln\xi(t)\,. \tag{6}$$

It is obvious that virtual time s in (6) can be controlled by ξ and never goes backward against actual time t. Thus, this virtual time s is used as a new time scale in this paper.

3.2 Time scaled artificial potential field

The kimenatic system of the robot can be described as

$$\dot{\boldsymbol{X}} = \boldsymbol{G}(\boldsymbol{X})\boldsymbol{U}, \tag{7}$$

where $\boldsymbol{X} \in \Re^n$ is the position vector of the robot; $\boldsymbol{U} \in \Re^n$ is the input vector; and it is assumed that $\det \boldsymbol{G}(\boldsymbol{X}) \neq 0$. The system given in (7) can be rewritten in virtual time s defined by (6) as follows:

$$\frac{d\boldsymbol{X}}{ds} = \frac{d\boldsymbol{X}}{dt}\frac{dt}{ds} = \boldsymbol{G}(\boldsymbol{X})\boldsymbol{U}_s, \tag{8}$$

where

$$\boldsymbol{U}_s = \frac{1}{a(t)}\boldsymbol{U}. \tag{9}$$

On the other hand, in the APFA [7] [8], the goal is represented by an artificial attractive potential field depends on the defined potential function $V(\boldsymbol{X})$ in the task space. The potential function $V(\boldsymbol{X})$ has the minimum value $V(\boldsymbol{X}_d) = 0$ at the target point $\boldsymbol{X}_d$, so that

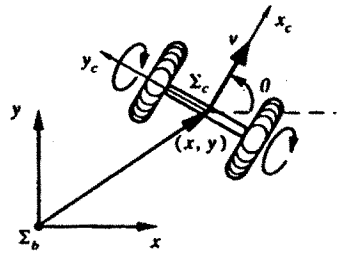

Fig.4 Model of a model car with two wheels

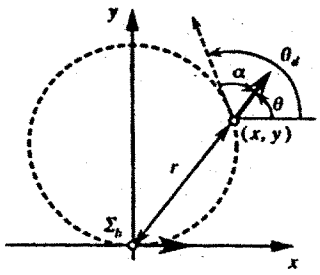

Fig.5 Coordinate transformation

the trajectory to the target can be generated by tracking a unique flow-line of the gradient field through the initial position. By using the inverse time-scaling from virtual time s to actual time t for the feedback controller U_s designed by the APFA, the feedback control law U in actual time t is derived as

$$U = -a(t)G^{-1}(X)\frac{\partial V}{\partial X}. \tag{10}$$

With the derived controller U, the system (7) in the actual time scale can be stable to the equilibrium point at the specified time t_f. In this paper, we attempt to generate the human-like trajectory for the robots by using the TBG based controller.

3.3 Trajectory generation of nonholonomic vehicle

In this subsection, with the TBG based method, a feedback control law which can generate a spatio-temporal trajectory of the model car is designed on the basis of the observed features of the experimental results with the subjects.

Figure 4 shows a model of the unicycle-like car which a subject manipulates in the experiment. Σ_b denotes the world coordinate system (for an operational space), and Σ_c is the moving coordinate system whose origin is set at the center of two wheels of the car and the x_c axis is oriented along the direction of motion of the car. Thus, the following generalized coordinates of the vehicle can be chosen: position (x, y) and orientation angle θ of Σ_c with respect to Σ_b.

The kinematics of the car can be described by the following relationship between the time derivative of $\boldsymbol{x} = (x, y, \theta)^T$ and the linear and the angular velocity of the car $\boldsymbol{u} = (v, \omega)^T$:

$$\dot{\boldsymbol{x}} = \boldsymbol{g}(\boldsymbol{x})\boldsymbol{u}, \tag{11}$$

where

$$\boldsymbol{g}(\boldsymbol{x}) = \begin{bmatrix} \cos\theta & 0 \\ \sin\theta & 0 \\ 0 & 1 \end{bmatrix}. \tag{12}$$

From the system equation (11), the following kinematic constraint can be easily derived [7]:

$$\dot{x}\sin\theta - \dot{y}\cos\theta = 0. \tag{13}$$

Therefore, there is the nonholonomic constraint given by (13) imposed on the hand movement of the subject in the process of manipulating the car.

In order to control the system, we adopt the piecewise smooth feedback control law proposed by Canudas de Wit and Sørdalen [13] which uses the family of circles that pass through the origin and the current position of the car and contact with the x axis at the origin as shown in Fig. 5. In the figure, θ_d belonging to $[-\pi, \pi)$ represents the tangential direction of this circle at the position x.

Let α denote the angle between the tangential direction θ_d and the current angular orientation θ with the intention of designing a control law which can eliminate this kind of *orientational error* together with the corresponding *positional error* denoted by the distance r from the target. The following coordinate transformation from $\boldsymbol{x} = (x, y, \theta)^T$ to $\boldsymbol{z} = (r, \alpha)^T$ is then introduced [7]:

$$r(x, y) = \sqrt{x^2 + y^2}, \tag{14}$$

$$\alpha(x, y, \theta) = e + 2n(e)\pi, \tag{15}$$

$$e = \theta - \theta_d, \tag{16}$$

$$\theta_d = 2\mathrm{atan2}(y, x), \tag{17}$$

where $n(e)$ is a function that takes an integer in order to satisfy $\alpha \in [-\pi, \pi)$. Also, $\mathrm{atan2}(\cdot, \cdot)$ is the scalar function defined as $\mathrm{atan2}(a, b) = \arg(b + ja)$, where j denotes the imaginary unit and arg denotes the argument of a complex number. As a result, the current state of the car can be represented by

$$\boldsymbol{z} = \boldsymbol{F}(\boldsymbol{x}) = \begin{bmatrix} r(x, y) \\ \alpha(x, y, \theta) \end{bmatrix}, \tag{18}$$

and the target configuration of the car is transformed from $\boldsymbol{x}_d = (0, 0)^T$ to $\boldsymbol{z}_d = (0, 0)^T$.

Substituting (11) into the time derivation of equation (18), the relationship between $\dot{\boldsymbol{z}}$ and the system input $\boldsymbol{u}$ can be derived as

$$\dot{\boldsymbol{z}} = \boldsymbol{J}(\boldsymbol{x})\boldsymbol{g}(\boldsymbol{x})\boldsymbol{u} = \boldsymbol{B}(\boldsymbol{x})\boldsymbol{u}, \tag{19}$$

where

$$\boldsymbol{J}(\boldsymbol{x}) = \begin{bmatrix} \frac{x}{\sqrt{(x^2+y^2)}} & -\frac{y}{\sqrt{(x^2+y^2)}} & 0 \\ \frac{2y}{x^2+y^2} & -\frac{2x}{x^2+y^2} & 1 \end{bmatrix}, \tag{20}$$

$$\boldsymbol{B}(\boldsymbol{x}) = \begin{bmatrix} b_1 & 0 \\ b_2 & 1 \end{bmatrix}, \tag{21}$$

$$b_1 = -(x\cos\theta + y\sin\theta)(x^2+y^2)^{-1/2}, \quad (22)$$

$$b_2 = 2(y\cos\theta - x\sin\theta)(x^2+y^2)^{-1}. \quad (23)$$

It can be seen that the number of state variables is reduced to the same number as the system input. For this system, the following potential function V so as to design the feedback controller can be defined:

$$V = \frac{1}{2}\left(k_r r^2 + k_\alpha \alpha^2\right), \quad (24)$$

where k_r and k_α are positive constants.

From (10), the feedback controller $\boldsymbol{u}$ based on the potential function V (24) can be designed as

$$\boldsymbol{u} = -\frac{1}{2}a(t)\boldsymbol{B}^{-1}(\boldsymbol{x})\frac{\partial V}{\partial \boldsymbol{z}} = \begin{bmatrix} \frac{k_r p r \dot{\xi}}{2b_1\xi} \\ -b_2 v + \frac{k_\alpha p \alpha \dot{\xi}}{2\xi} \end{bmatrix} \quad (25)$$

under the assumption of $\det \boldsymbol{B}(\boldsymbol{x}) \neq 0$ except at the target position $\boldsymbol{x}_d$. With the feedback controller $\boldsymbol{u}$, the time derivative of V yields

$$\dot{V} = \left(\frac{\partial V}{\partial \boldsymbol{z}}\right)^T \boldsymbol{B}(\boldsymbol{x})\boldsymbol{u} = pV\frac{\dot{\xi}}{\xi} < 0. \quad (26)$$

As $\dot{V}$ is always negative except at the equilibrium point, the system of the car in the actual time scale is asymptotically stable by means of the designed feedback control law $\boldsymbol{u}$. Moreover, this differential equation given in (26) can be readily solved as follows [8]:

$$V = V_0 \xi^p, \quad (27)$$

where $V_0 = V(\boldsymbol{x}_0)$ is the initial value of V. It can be seen that the potential function V is "synchronized" with the TBG because V is proportional to the pth power of ξ. Since ξ reaches zero at t_f so must do V: in other words, the car with two wheels is bound to reach the target position $\boldsymbol{x}_d$ from the initial position $\boldsymbol{x}_0$ just at $t = t_f$ with the controller $\boldsymbol{u}$.

4 Computer simulations

In this section, the human-like trajectories for the robots whose velocity profiles are single or double-peaked is generated by means of the designed controller (25). In the simulations explained below, the target posture is $\theta_d = \pi$ [rad] with the convergence time $t_f = 2.5$ [s] under the parameters $p = 2.0$, $k_r = k_\alpha = 1.0$. The TBG parameters, β_1, β_2, are changed according to the generating spatial trajectory so as to regulate the temporal trajectory.

4.1 Trajectory generation with single-peaked velocity profile

Figure 6 shows generated primitive trajectories with single-peaked profile and switching trajectories with the different initial positions $\boldsymbol{x}_0 = (0.6, 0.6)^T$, $(0.2, 0.6)^T$, $(0.2, 0.2)^T$, $(0.6, 0.2)^T$ [m] under the initial direction $\theta_0 = \frac{\pi}{2}$ [rad]. The target points is set at $\boldsymbol{x}_d = (0.4, 0.4)^T$ [m]. Here, in generating the trajectory ① and ③, the virtual targets as switching points

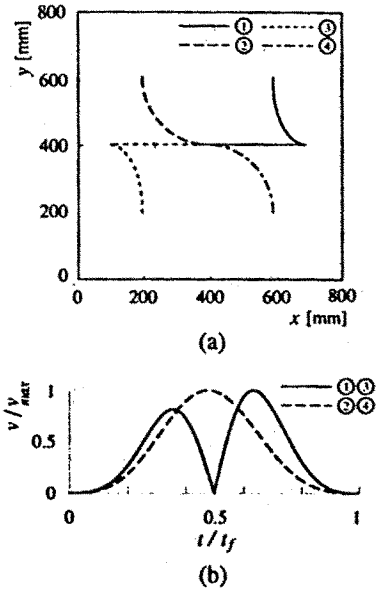

Fig.6 Generated trajectories with single-peaked velocity profiles

were set at $\boldsymbol{x}_v^* = (0.7,\ 0.4)^T$, $(0.1,\ 0.4)^T$ [m], respectively, and two primitive trajectories with single-peaked profiles, which are separately generated before and after the switching time $t = \frac{t_f}{2}$, were connected at the given virtual target.

In the time histories of the velocity (Fig. 6 (b)), the vertical axis is normalized by the maximum velocity v_{max} for each trial, and the horizontal axis by the specified time $t_f = 2.5$ [s], respectively. It can be seen that the generated quadrantal-arc trajectories ②, ④ have single-peaked velocity profiles all which takes the maximum value at $t = \frac{t_f}{2}$. Comparing the trajectories ① and ③ with the human switching trajectories in Fig. 2 (b), it can be also observed that the generated switching trajectories have the same characteristics as human ones have. The designed controller with the TBG can generate spatio-temporal trajectories which are similar to human trajectories.

4.2 Trajectory generation with double-peaked velocity profile

In order to generate a curved trajectory, a via-point $\boldsymbol{x}_v^*$ and a via-orientation $\theta_v^* = \mathrm{atan2}(y_v^*,\ x_v^*)$ are set in the task space, which moves to the targets from $t = t_i^a$ to $t = t_i^b$ $(i = x, y, \theta)$ smoothly.

Figure 7 shows the generated trajectories with the initial position $(\boldsymbol{x}_0,\ \theta_0) = (0.7$ [m], 0.4 [m], π [rad]$)^T$ and the target point $\boldsymbol{x}_d = (0.1,\ 0.4)^T$ [m]. For the curved spatial trajectories ②, ③ in Fig. 7 (a), the via-points were set at $\boldsymbol{x}_v^* = (0.4,\ 0.6)^T$, $(0.4,\ 0.7)^T$ [m], respectively. Also, t_i^a and t_i^b were set empirically with respect to the specified time t_f as follows: $t_x^a = t_y^a = 0.35t_f$, $t_\theta^a = 0.1t_f$, $|t_i^a - t_i^b| = \frac{t_f}{2}$. Figure 7 (b) shows the normalized velocity profiles for each

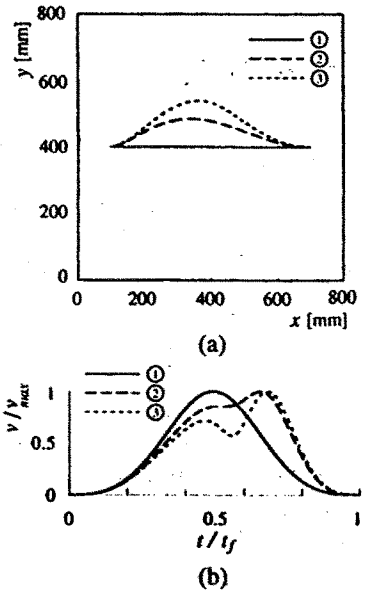

Fig.7 Generated trajectories with single-peaked and double-peaked velocity profiles

generated spatial trajectory.

It can be observed from Fig. 7 that the generated curved spatio-trajectories have the double-peaked velocity profiles sinking around $t = \frac{t_f}{2}$. Also, as the amplitude of the curvature becomes to be larger, the velocity profile tends to be more sharply double-peaked. Owing to setting the via-point in the task space, the generated curved trajectories with double-peaked velocity profiles are in good agreement with the observed human trajectories.

5 Conclusions

In this paper, we try to generate the trajectories on the nonholonomic constrained task for the robots by imitating human generated trajectories. By applying the TBG based method with the concept of via-point and virtual target, we could generate the trajectories which have similar features of the observed human trajectories.

Future research will be directed to investigate the influence of constraints for human arm movements with other experimental conditions and constrained tasks, and to develop a motion planning method for generating the same spatio-temporal trajectory depending on specified conditions as a human does.

Acknowledgment This work was partly supported by the Scientific Research Foundation of the Ministry of Education, Science, Sports and Culture, Japan (11555113 and 11650450).

References

[1] K. Hirai, M. Hirose, Y. Haikawa and T. Takenaka: "The development of Honda humanoid robot," in Proceedings of IEEE Int. Conf. on Robotics and Automation, pp. 1321–1326, 1998.

[2] P. Morasso: "Spatial control of arm movements," Experimental Brain Research, 42, pp. 223–227, 1981.

[3] T. Flash and N. Hogan: "The coordination of arm movements: An experimentally confirmed mathematical model," Biological Cybernetics, Vol. 57, pp. 1688–1703, 1985.

[4] Y. Uno, M. Kawato and R. Suzuki: "Formation and control of optimal trajectory in human multi-joint arm movement," Biological Cybernetics, Vol. 61, pp. 89–101, 1989.

[5] D. Bullock and S. Grossberg: "VITE and FLETE: Neural modules for trajectory formation and postural control," in Volitional Action (W. A. Hershberger, Ed.), pp. 253–297, Amsterdam, (Elsevier, North-Holland), 1989.

[6] P. Morasso, V. Sanguineti and T. Tsuji: "A dynamical model for the generator of curved trajectories," in Proceedings of the International Conference on Artificial Neural Networks, pp. 115–118, 1993.

[7] T. Tsuji, P. Morasso and M. Kaneko: "Feedback control of nonholonomic mobile robots using time base generator", in Proceedings of IEEE Int. Conf. on Robotics and Automation, pp. 1385–1390, 1995.

[8] T. Tsuji, P. Morasso, V. Sanguineti, and M. Kaneko: "Artificial force-field based methods in robotics," in Self-Organization, Computational Maps and Motor Control (P. Morasso and V. Sanguineti, Ed.), Advances in Psychology, 119, pp. 169-190, (Elsevier, North-Holland), 1997 .

[9] Y. Tanaka, T. Tsuji, M. Kaneko and Pietro G. Morasso: "Trajectory generation using time scaled artificial potential field," in Proceedings of IEEE/RSJ Int. Conf. on Intelligent Robots and Systems, pp.223 - 228, 1998.

[10] Y. Tanaka, T. Tsuji, M. Kaneko: "Trajectory formaion of human arm with nonholonomic constraints," in Proceedings of 3rd International Conference on Advanced Mechatronics, Vol.2, pp.1 - 6, 1998.

[11] D. A. Winter: "Biomechanics and motor control of human movement (2nd ed.)," Jhon Wiley and Son's Inc. , New York, pp. 41–43, 1990.

[12] M. Sampei and K. Furuta: "On time scaling for nonlinear systems: Application to linearization," IEEE Transactions on Automatic Control, Vol. 31, No. 5, pp. 459–462, 1986.

[13] C. Canudas de Witt and O.J.Sørdalen: "Exponential stabilization of mobile robots with nonholonomic constraints", IEEE Transactions on Automatic Control, Vol. 37, No. 11, pp. 1791–1797, 1992.